
Convex Max-Product Algorithms for Continuous MRFs with Applications to Protein Folding

Jian Peng
Tamir Hazan
David McAllester
Raquel Urtasun

TTI Chicago, Chicago

PENGJIAN@TTIC.EDU
TAMIR@TTIC.EDU
MCALLESTER@TTIC.EDU
RURTASUN@TTIC.EDU

Abstract

This paper investigates convex belief propagation algorithms for Markov random fields (MRFs) with continuous variables. Our first contribution is a theorem generalizing properties of the discrete case to the continuous case. Our second contribution is an algorithm for computing the value of the Lagrangian relaxation of the MRF in the continuous case based on associating the continuous variables with an ever-finer interval grid. A third contribution is a particle method which uses convex max-product in re-sampling particles. This last algorithm is shown to be particularly effective for protein folding where it outperforms particle methods based on standard max-product resampling.

1. Introduction

Many applications such as protein folding (Sontag & Jaakkola, 2009) and stereo vision (Trinh & McAllester, 2009) can be formulated as an inference problem in a graphical model. A graphical model assigns an energy or (equivalently) a probability to each assignment of values to a given set of variables. Inference algorithms can be divided into those that attempt to compute marginal distributions on single variables or small subsets of variables and those that attempt to find global assignments minimizing energy, or equivalently, maximizing probability. Here we focus on inference algorithms of the latter form — we seek the minimum energy configuration of a set of variables under locally defined potential functions.

Recently there has been considerable success in finding minimum-energy configurations using a method

known as convex belief propagation (BP) (Globerson & Jaakkola, 2007; Sontag et al., 2008; Sontag & Jaakkola, 2009). This approach can be formulated in terms of a linear programming (LP) relaxation of the (typically NP hard) minimum-energy problem. One works with the dual of the LP relaxation where the dual variables can be interpreted as messages between cliques (local energy terms). A message passing algorithm can be formulated in which the dual variables are updated using a form of block coordinate ascent. This dual algorithm is surprisingly similar to classical max-product message passing algorithms. However, the dual of the LP relaxation provides a simple concave objective function being optimized by the message-passing process where the value of this objective is a lower bound on the original problem. Hence the term “convex BP”.

Convex BP has been formulated for graphical models with discrete variables each with a finite number of values. Here we are interested in finding ways of applying convex BP to models with continuous variables. For graphical models with continuous variables the LP relaxation is awkward to define. In the discrete case the LP relaxation involves a variable for each value of each discrete variable. If the variables take on real values then we get continuum-many variables in the LP relaxation. In the continuous case convex BP involves messages which are functions of continuous variables.

The first contribution of this paper is a proof that certain basic properties of convex relaxations of MRFs apply to the continuous case as well as the discrete case, provided that the continuous variables are a priori bounded and the local potential functions are continuous. We show that under these conditions the optimum of the Lagrangian relaxation can be realized at a setting of the dual variables to continuous (as opposed to arbitrary) functions. Furthermore, a setting of the dual variables to continuous functions achieves an optimal value when the corresponding primal values are unique (the clique potentials have no ties).

Appearing in *Proceedings of the 28th International Conference on Machine Learning*, Bellevue, WA, USA, 2011. Copyright 2011 by the author(s)/owner(s).

Our second contribution is an algorithm for computing the value of the Lagrangian relaxation of the MRF in the continuous case based on associating the continuous variables with an ever-finer interval grid. While this algorithm provably converges to the correct value, it is not practical for relative large problems such as those that arise in protein folding.

The last contribution is a convex max-product particle method which, while it is susceptible to local optima, performs very well in practice. We demonstrate the effectiveness of our approach in the task of protein folding and show that our particle method significantly outperforms particle max-product as well as discrete convex max-product. We also show that while using a very simple energy function we perform comparably to the state-of-the-art (Sali & Blundell, 1993) which takes into account a larger set of physical constraints derived from prior knowledge.

2. Related Work

In recent years there has been a large body of work in message-passing frameworks for continuous and discrete variables. The max-product algorithm is known to solve exactly arbitrary programs on trees (Weiss & Freeman, 2001). However, as demonstrated in our experiments, when the graph contains cycles it is not guaranteed to converge and may produce suboptimal solutions. Max-product was also successfully applied to quadratic programs in the context of Gaussian graphical models (Bickson, 2008). In contrast, we consider arbitrary continuous functions over compact sets.

Non parametric sum-product (Sudderth et al., 2010) parametrized the messages for arbitrary functions with mixture of Gaussians. Unfortunately, there are no guarantees that it can produce optimal solutions as mixtures of Gaussians cannot accurately represent the space of possible messages. Particle sum-product (Ihler & McAllester, 2009) replaced the message representation with samples, i.e., particles. Particle sum-TRBP replaced the Bethe entropy with the TRW entropy (Ihler et al., 2009). These approaches differ from ours in several important aspects: First, our algorithm is a max-product algorithm instead of sum-product, as we are motivated by the MAP problem in protein folding. We believe max-product solvers are a better choice as they inherently focus on point-mass distributions, thus less information is needed to represent their states in continuous spaces. Moreover, as our approach is defined on compact sets, the space we need to represent the messages is reduced.

Particle max-product was introduced by (Trinh &

McAllester, 2009). Our particle algorithm uses the convex form of max-product and as demonstrated in our experiments this difference is very important in practice as particle max-product is very sensitive in problems with many degrees of freedom.

This paper is a continuation of a line of work on convex max-product for the MAP assignment problem (Schlesinger, 1976; Werner, 2007; Sontag & Jaakkola, 2009; Meltzer et al., 2009; Hazan & Shashua, 2010). In contrast, we constrain our derivation to compact sets and exploit strong duality to improve the conditions in the recovery of the optimal solution (see Claim 1).

3. A Review on Convex Max-Product

A graphical model assigns an energy, or equivalently a probability, for every assignment to the system variables. These graphical models typically consider two types of functions: the first are functions over a single variable which correspond to the vertices in the graph, i.e., $\theta_i(x_i)$. The second are functions of the form $\theta_\alpha(x_\alpha)$ which are defined over subsets of variables $\alpha \subset \{1, \dots, n\}$ and correspond to the graph hyperedges. In this paper we focus on the MAP estimation problem, which attempts to find an assignment that maximizes the probability, or minimizes the energy, and consider the setting where the random variables are either discrete or bounded continuous. Estimating the MAP can be written as a program of the form:

$$\operatorname{argmin}_{x_1, \dots, x_n} \sum_{i \in V} \theta_i(x_i) + \sum_{\alpha \in E} \theta_\alpha(x_\alpha). \quad (1)$$

Note that these programs are extensively used in learning and inference. Solving these programs is in general computationally challenging: when restricted to Euclidean spaces only local minimum can be found, and when restricted to discrete spaces, the program is NP-hard (Shimony, 1994).

Recent developments introduced message-passing solvers for graphical models based on maximizing a lower bound of (1), constructed via a reparameterization (Sontag & Jaakkola, 2009; Meltzer et al., 2009). This lower bound can be derived by adding and subtracting $\sum_{\alpha, i \in N(\alpha)} \lambda_{i \rightarrow \alpha}(x_i)$ to the program in (1), followed by commuting minimization with summation, namely

$$\inf_x \left\{ \sum_{\alpha \in E} \theta_\alpha(x_\alpha) + \sum_{i \in V} \theta_i(x_i) + \sum_{\alpha, i \in N(\alpha)} \lambda_{i \rightarrow \alpha}(x_i) - \sum_{i, \alpha \in N(i)} \lambda_{i \rightarrow \alpha}(x_i) \right\} \geq \sum_{\alpha \in E} \inf_{x_\alpha} \{ \theta_\alpha(x_\alpha) + \sum_{i \in N(\alpha)} \lambda_{i \rightarrow \alpha}(x_i) \} + \sum_{i \in V} \inf_{x_i} \{ \theta_i(x_i) - \sum_{\alpha \in N(i)} \lambda_{i \rightarrow \alpha}(x_i) \} \quad (2)$$

This function is concave as it is the pointwise infimum of linear functions in $\lambda_{i \rightarrow \alpha}$. Moreover, iteratively increasing the value of this lower bound is guaranteed to converge. A family of max-product algorithms, shown

Algorithm 1 Convex Max-Product:

Set $\hat{c}_i = c_i + \sum_{\alpha \in N(i)} c_\alpha$. For every $i = 1, \dots, n$ repeat until convergence: $\forall \alpha \in N(i), x_i$:

$$\begin{aligned} \mu_{\alpha \rightarrow i}(x_i) &= \inf_{x_\alpha \setminus x_i} \left\{ \theta_\alpha(x_\alpha) + \sum_{j \in N(\alpha) \setminus i} \lambda_{j \rightarrow \alpha}(x_j) \right\} \\ \lambda_{i \rightarrow \alpha}(x_i) &= \frac{c_\alpha}{\hat{c}_i} \left(\theta_i(x_i) + \sum_{\beta \in N(i)} \mu_{\beta \rightarrow i}(x_i) \right) - \mu_{\alpha \rightarrow i}(x_i) \end{aligned}$$

in Algorithm 1, can be applied to iteratively maximize the concave program in (2) when the variables are either discrete or continuous. These algorithms increase the lower bound whenever $c_i, c_\alpha > 0$, however finding the best c_α, c_i is an open problem. This algorithm reduces to the max-product algorithm when using the Bethe entropy, i.e., $c_\alpha = 1, c_i = 1 - |N(i)|, \hat{c}_i = 1$. In this case $c_i < 0$, and the algorithm is not guaranteed to improve the lower bound nor to converge when dealing with graph with cycles. This algorithm is typically used in the discrete case. In the continuous case, computing the supremum is computationally intractable, as the θ functions are arbitrary.

4. Convex Max-Product for Discrete and Bounded Continuous Variables

In this section we first show that the dual optimal solution, for discrete and continuous bounded variables, can be obtained using continuous functions and derive the sufficient conditions for optimality, as well as for recovering the MAP assignment. We then derive an algorithm which we called interval convex max-product, which maximizes a lower bound of the energy in (2), which is created by associating each real-value variable with a finite set of intervals, and then formulating a discrete problem where for each interval we bound the best case energy. Finally, we derive an effective particle convex max-product method, where each variable is associated with a discrete set of possible values.

4.1. Theoretical Properties

The main problem when using the max-product program in (2) is recovering the MAP assignment from the optimal dual solution. (Weiss et al., 2007) showed that an optimal solution for a max-product type program corresponds to the MAP assignment if the minimum arguments x_i^*, x_α^* are consistent. In this work, we extend (Weiss et al., 2007) and describe for general programs with discrete and bounded continuous variables the conditions under which the max-product

program achieves optimal dual messages, as well as sufficient conditions for which it can recover the MAP assignment. In order to derive these conditions we rely on duality between continuous functions and regular Borel measures over compact spaces.

We begin by transforming the program in (1) into a linear program over the continuous functions θ_i, θ_α subject to non-convex constraints, and then derive its dual. We use the bracket notation $\langle \theta, \delta \rangle$ to denote the linear function δ over the Banach space of continuous functions $\theta(x)$, keeping in mind that both θ and δ may not be vectors, or come from the same Banach space. Let K_i be the compact set of x_i and let K_α be the Cartesian product of the compact sets K_i over $i \in N(\alpha)$. The objective in (1) can be described by the linear function $\sum_\alpha \langle \theta_\alpha, \cdot \rangle + \sum_i \langle \theta_i, \cdot \rangle$. The continuous linear functions over θ_α, θ_i are identified with the set of regular Borel measures over the compact sets K_α and K_i (Rockafellar, 1974). We use point mass measures, i.e., probability measures that concentrate all their weight on a single point, to formulate the program in (1) as

$$\min_{\delta_i, \delta_\alpha} \sum_\alpha \langle \theta_\alpha, \delta_\alpha \rangle + \sum_i \langle \theta_i, \delta_i \rangle \quad (3)$$

subject to:

δ_i, δ_α are point mass probability measures

$$\forall i, x_i, \alpha \in N(i), \int_{x_\alpha \setminus x_i} \delta_\alpha(x_\alpha) = \delta_i(x_i)$$

Note that we have traded the computational complexity of the objective in (1) with the one of the feasible set in (3), thus the computational complexity remains high. As the set of all point mass measures is not convex, this linear program cannot be efficiently solved in general, e.g., when all compact sets are discrete, the feasible set consists of zero-one variables and the program in (3) reduces to an integer linear program.

In the following, we make the program in (3) concave by constructing its dual. We expect to recover the MAP solution when the dual optimal solution does not have a duality gap. Geometrically, the dual variables are hyperplanes that support the set whose elements have the form $(\delta, \langle \delta, \theta \rangle)$, where δ is a measure of the form $(\int \delta_\alpha - \delta_i)_{i, \alpha \in N(i)}$ and $\langle \delta, \theta \rangle$ is the linear objective in (3). The duality between regular Borel measures and continuous functions on compact sets implies that the hyperplanes $\lambda_{i \rightarrow \alpha}$ are continuous functions. The dual function $q(\lambda)$ describes the offset of a $(\lambda, 1)$ -slope hyperplane that support the set $(\delta, \langle \delta, \theta \rangle)$, therefore the dual value is obtained by minimizing the

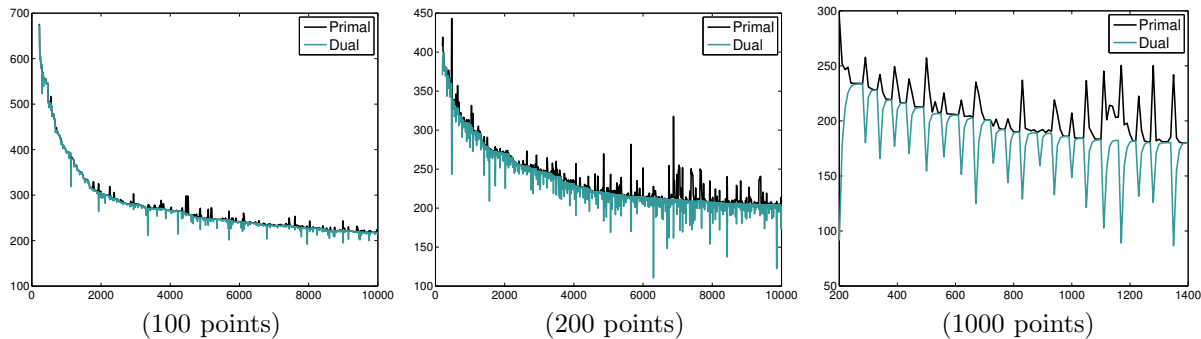


Figure 1. **Primal and dual objective** for sampling sets of different sizes. Picks in the objectives are due to resampling. Note that in most of the cases for a fix sample set the algorithm converges with no ties as there is no primal dual gap. More importantly, the different steps in the resampling act as tightening and the primal objective decrease over time.

Lagrangian with respect to point mass distributions:

$$q(\lambda) = \inf_{\delta_i, \delta_\alpha} \left\{ \langle \theta, \delta \rangle + \sum_{i, \alpha \in N(i)} \langle \lambda_{i \rightarrow \alpha}, \int \delta_\alpha - \delta_i \rangle \right\}.$$

Since the point mass measures are concentrated around a single point in the compact space and the functions are continuous, this infimum is always attained and the dual function takes the form:

$$q(\lambda_{i \rightarrow \alpha}) = \sum_{\alpha} \min_{x_{\alpha} \in K_{\alpha}} \left\{ \theta_{\alpha}(x_{\alpha}) + \sum_{i \in N(\alpha)} \lambda_{i \rightarrow \alpha}(x_i) \right\} + \sum_i \min_{x_i \in K_i} \left\{ \theta_i(x_i) - \sum_{\alpha \in N(i)} \lambda_{i \rightarrow \alpha}(x_i) \right\} \quad (4)$$

This dual program is an instance of the lower bound in (2) restricted to compact sets and continuous functions. The main difference is that the strong duality theorem guarantees that the optimum of the bound can be achieved when restricted to continuous functions $\lambda_{i \rightarrow \alpha}(x_i)$.

Our goal is to find a dual optimal solution and to use it in order to recover the MAP assignment for (1). This cannot be done in all cases: Convex max-product algorithms minimize non-smooth functions, thus it might converge to a corner which is not dual optimal. Moreover, since the dual program is a concave relaxation of the MAP program, convex max-product can reach a dual optimal point which has a duality gap from the MAP optimum. We now derive optimality conditions, as well as describe the conditions for which the dual optimal solution can produce the MAP assignment.

Claim 1 Let X_i^* and X_{α}^* be the sets of all optimal

solutions defined as

$$X_i^* = \operatorname{argmin}_{x_i} \{ \theta_i(x_i) - \sum_{\alpha \in N(i)} \lambda_{i \rightarrow \alpha}(x_i) \}$$

$$X_{\alpha}^* = \operatorname{argmin}_{x_{\alpha}} \{ \theta_{\alpha}(x_{\alpha}) + \sum_{i \in N(\alpha)} \lambda_{i \rightarrow \alpha}(x_i) \}.$$

If there exist probability measures b_{α}, b_i whose supports are contained in X_{α}^*, X_i^* and they agree on their marginals, then the continuous functions $\lambda_{i \rightarrow \alpha}(x_i)$ are dual optimal. If b_{α}, b_i are point mass distribution then they point towards an optimal MAP assignment. In particular, if the functions $\theta_i(x_i) - \sum_{\alpha \in N(i)} \lambda_{i \rightarrow \alpha}(x_i)$ have no ties (i.e., X_i^* is a singleton) then x_1^*, \dots, x_n^* is the MAP assignment.

Proof: The first claim follows from the strong duality theorem for regular Borel measures and continuous functions on compact sets, cf. Theorem 6 (Rockafellar, 1974). If b_{α}, b_i are point mass measures, we set x_i^* to be the point indicated by b_i . Assigning x_1^*, \dots, x_n^* as the minimal arguments in the dual objective in (4), we recover the MAP objective in (1) as the messages cancel out. Since the dual lower bounds the primal in (3) the second claim follows. If $\theta_i(x_i) - \sum_{\alpha \in N(i)} \lambda_{i \rightarrow \alpha}(x_i)$ has no ties after convergence, then b_i is a point mass distribution. Since b_{α} agree with b_i on its marginal distributions it follows that b_{α} is a point mass distribution, and the third claim follows. \square

4.2. Interval Convex Max-Product

The second contribution of this paper is an algorithm that we call *interval convex max-product* for solving the dual program in (2). The algorithm associates each bounded real-valued variable x_i with a finite set \mathcal{I}_i of disjoint (possibly open or half open) intervals whose union covers the (bounded) range of x_i . Initially \mathcal{I}_i consists of the single closed interval which is the entire range of x_i . We let \bar{x} denote an assignment of an interval $\bar{x}_i \in \mathcal{I}_i$ to each variable x_i . We

let \bar{x}_α be the restriction of \bar{x} to the variables in hyperedge α and write $x_\alpha \in \bar{x}_\alpha$ to mean that $x_i \in \bar{x}_i$ for each i in α . We construct the potential functions $\bar{\Phi}_i(\bar{x}_i)$ and $\bar{\Phi}_\alpha(\bar{x}_\alpha)$ with $\bar{\Phi}_i(\bar{x}_i) \leq \Phi(x_i)$ for $x_i \in \bar{x}_i$ and $\bar{\Phi}_\alpha(\bar{x}_\alpha) \leq \Phi(x_\alpha)$ for $x_\alpha \in \bar{x}_\alpha$. The potential functions must also have the property that in the limit of small ϵ we have that $\bar{\Phi}_i([x_i, x_i + \epsilon])$ approaches $\Phi(x_i)$. This can be achieved with interval evaluation of the potential functions. This defines the discrete MRF $\min_{\bar{x}} \sum_i \bar{\Phi}_i(\bar{x}_i) + \sum_\alpha \bar{\Phi}_\alpha(\bar{x}_\alpha)$. Because the potential functions have been defined optimistically, the value of this discrete MRF is a lower bound on the value of the original continuous MRF. We can use a convex max-product algorithm to compute the value of the Lagrangian relaxation of this discrete MRF. We can also recover primal values which, in general, give for each variable x_i a probability distribution over the intervals in \mathcal{I}_i for x_i . We then refine the intervals by splitting each interval which is assigned a nonzero probability, focusing the interval refinement on promising intervals. This process of interval refinement results in a series of discrete MRFs. One can show that for bounded continuous variables and continuous potential functions the values of the Lagrangian relaxations of this series of discrete problems approaches the value of the continuous Lagrangian relaxation (2). The interval algorithm can also be interpreted as an instance of convex max-product for the original continuous problem but where the messages are restricted to be piecewise constant functions on the given set of intervals. While this algorithm provably converges to the correct value, it is not practical for real-world applications.

4.3. Particle Convex Max-Product

The third contribution of this paper is an algorithm that we call *particle convex max-product*. In particle methods each variable is associated with a discrete set of possible values (point values rather than intervals) (Koller et al., 1999; Ihler & McAllester, 2009). Given a set of particles, one considers a discrete model where the particles define the set of possible values for each variable. Particle convex max-product alternates between computing the MAP assignment for each variable using convex max-product on the discrete problem defined by the particles, and re-sampling to get new particles. This is similar in spirit to particle filters but with the re-sampling done many times across the whole network. In particular, we proposed to re-sample around the sets X_i^* defined in Claim 1. This is summarized in Algorithm 2

Unfortunately, the particle convex max-product is a local search method and does not yield a lower bound on the minimal energy. However, as demonstrated below

Algorithm 2 Particle convex max-product:

Sample finite number of points for the sets X_1, \dots, X_n .
Repeat until convergence:

1. Run convex max-product on the discrete sets X_1, \dots, X_n until convergence.
 2. Set $X_i^* = \operatorname{argmin}_{x_i} \{\theta_i(x_i) - \sum_{\alpha \in N(i)} \lambda_{i \rightarrow \alpha}(x_i)\}$.
Resample X_i around the points in X_i^* .
-

Table 1. Influence of the sample size: When using larger sample sizes the primal value obtained is better but the computational complexity increases and the algorithm is slower to converge (in time). Note however, that it requires much smaller number of iterations.

# sampling points	100	200	1000
sampling iters	315	238	30
total iters	10000	8800	1400
total time	9.16	13.2	16.1
primal	217.72	204.18	180.28

particle convex max-product works very well in practice, significantly outperforming particle max-product for the problem of protein folding.

5. Protein structure prediction

Predicting the 3D structure of a protein from a sequence of amino acids is one of the grand challenges in computational biology. Template-based approaches build the 3D structure of a protein by aligning the query to a set of templates with known 3D structure. These approaches have been shown to be very effective if at least one of the templates is close to the query structure (Cozzetto et al., 2009). Additionally, physical constraints such as local spatial constraints on consecutive residues (e.g. bond lengths and angles should be valid) as well as predicted contacts between two amino acids are typically imposed. However, the problem is hard to solve due to miss-alignments between the templates and the target proteins as well as the fact that each template might provide different distance constraints for a given amino acid pair. Most existing template-based approaches use Monte Carlo simulated annealing to find possible structures that satisfy most of these constraints (Simons et al., 1997; Sali & Blundell, 1993).

In this paper we focus on predicting the 3D coordinates of the C_α atoms in the protein backbone and show that, while only considering a subset of these constraints, accurate prediction can be performed. We employ distance constraints extracted from template structures and formulate the prediction as a discrete/continuous hybrid optimization problem. More formally, let x_1, \dots, x_n be variables representing the 3D

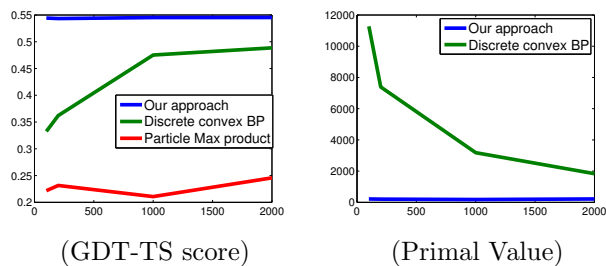


Figure 2. **Comparison to other inference approaches** in terms of (left) GDT-TS and (right) primal value. Our approach outperforms discrete convex max-product. Particle max product performs very poorly; Its primal value is omitted since it’s out of range.

coordinates of the C_α atoms of each amino acid in the query protein, and let D be the number of templates available for this protein. Template k provides a distance constraint, $d_{i,j}^k$, for the edge connecting nodes i and j if it covers both nodes, i.e., contains the corresponding amino acids. Let $T_{i,j} \subseteq \{1, \dots, D\}$ be the set of all possible choices of template for each pair of variables, with $T_{i,j}$ the empty set if there is no template covering the i -th and j -th node, and let $x_{ij} \in T_{i,j}$ be discrete variables representing these choices.

We can write the protein folding problem as

$$\min_{x_i \in \mathbb{R}^3, x_{ij} \in T_{i,j}} \sum_{i,j} \theta_{i,j}(x_i, x_j, x_{ij}) + \sum_i \theta_{i,i+1}(x_i, x_{i+1}) \quad (5)$$

where $\theta(x_i, x_{i+1})$ is defined to avoid the chain-break of the backbone structure by imposing a virtual bond length on consecutive atoms, and $\theta_{i,j}(x_i, x_j, x_{ij})$ exploits the templates in the form of distance constraints

$$\begin{aligned} \theta_{i,j}(x_i, x_j, x_{ij}) &= (\|x_i - x_j\| - d_{i,j}^{x_{ij}})^2 \\ \theta_{i,j}(x_i, x_{i+1}) &= (\|x_i - x_{i+1}\| - \beta)^2 \end{aligned}$$

where $d_{i,j}^{x_{ij}}$ is the pairwise distance extracted from the x_{ij} -th template if the corresponding amino acids are present in that template. We determined β by the nature conformation of peptide bonds to be $\beta = 3.8$. Protein folding can be interpreted as an optimization problem composed of continuous 3D variables x_i and discrete variables x_{ij} . The cliques have size three for the hybrid functions $\theta_{i,j}(x_i, x_j, x_{ij})$, and size two for the functions $\theta_{i,i+1}(x_i, x_{i+1})$ over the Euclidean space. Other scoring terms can also be incorporated but we only consider the distance constraints between C_α atoms in this work. In the next section we show that by employing our particle convex max-product scheme in these hybrid models, the 3D structures of a wide range of proteins can be accurately predicted.

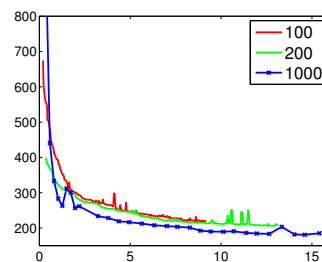


Figure 3. **Primal objective as a function of time** for different number of points in the resampling. Sampling with small sample sets is beneficial initially, but it is soon outperformed by sampling with larger sample sets.

Table 2. **Importance of the hybrid representation:** GDT-TS for protein *4icb* when using a single template (i.e., *1j7qa*) or multiple templates.

# templates	1	2
MODELLER	48.9	49.2
Our approach	52.8	54.4

6. Experimental Evaluation

We use the dataset of (Simons et al., 1997) as well as a subset of the recent CASP experiments (<http://predictioncenter.org/>) to evaluate the performance of our method. The dataset contains 20 proteins with size ranging from 43 to 186 amino acids. For each protein, one or two templates are identified. The alignments between query proteins and their templates are generated by BoostThreader (Peng & Xu, 2010), a protein threading algorithm. The number of cliques in the graphical model ranges from 788 to 16833. To avoid the inherent structure ambiguity, we fix the coordinates of the first four atoms to be the ones of the first template. To evaluate the distance between the predicted structure and the native structure (i.e., ground truth), we first superimpose the prediction and the native structure using the Kabsch algorithm (Kabsch, 1976). We then measure the quality of the prediction using the GDT-TS score (Zemla et al., 1999), which can be computed as the averaged percentage of correct aligned amino acids under distance cut-offs of 1Å, 2Å, 4Å and 8Å. We utilize this score as it is widely used to evaluate protein folding and it is used CASP.

We compare our approach to MODELLER (Sali & Blundell, 1993); which achieves state-of-art results in a wide range of proteins (Eswar et al., 2007). It is based on Monte Carlo simulated annealing with molecular dynamics applied to optimize the scoring function from spatial constraints. We also compare our approach to other MRF inference algorithms, including discrete convex max-product (Meltzer et al., 2009; Hazan & Shashua, 2009) and particle max-product

(Trinh & McAllester, 2009).

We first demonstrate the behavior of our approach using *4icb* (*Calbindin D9k*), a protein of size 76 with 2278 distance constraints (i.e., edges in the graph). This protein has two templates *1j7qa* and *2roba* found with fold-level similarity. Fig. 1 shows primal and dual values as a function of the number of iterations when resampling with different sample sizes. As expected when using a large number of samples only a few resampling iterations are required when compared with sampling with small sets. However, as shown in Fig. 3 each iteration is computationally more expensive when the sample size is large. The picks in the primal and dual objectives in Fig. 1 correspond to the iteration when the algorithm resamples. Note that in most cases, our approach converges without ties for each resampling step as there is no primal-dual gap. The different steps in the resampling act as tightening and the primal-dual objectives decrease over time.

Fig. 3 depicts the primal values achieved by our approach as a function of time for different sample sizes. Note that the curves are smooth as we only plot the primal values after convergence of each resampling iteration. Initially, sampling with small number of points gets faster to a good solution. However, very quickly in the optimization, sampling with more points outperforms sampling with fewer points. This suggests that a good strategy would be to use a small sample set to locate the region of interest and then use a larger set to get the best possible solution. Table 4.3 summarizes the influence of the sample size.

Fig. 2 depicts GDP-TS score as well as primal value on the *4icb* protein as a function of the number of particles for discrete convex max-product, particle max-product and our approach. As expected a fixed discretization is suboptimal when compared to our approach which uses the dynamics of the algorithm to decide where to sample. Particle max-product produces very bad estimates in terms of both the GDT-TS score and the primal value. Note that its primal value is not shown in the figure, as its value is much worse than both discrete convex max-product and our approach. We believe this is because max-product is an aggressive solver that converges very fast to a local solution. Since we do not have a good initialization, particle max-product produces suboptimal solutions. In contrast, our approach is more conservative and it is guaranteed to iteratively improve.

We investigate this behavior in the next experiments. We first set as labels for each x_i the set of 76 optimal points obtained by our approach, and apply max-product on this discrete graphical model. Max-

Table 3. **Interval Convex Max-product:** Dual value as a function of the resolution.

# voxels	2^3	10^3	15^3	resampling
dual	0	0	0.28	0.57
running time	48s	22m	58m	60s

product converged to a suboptimal solution of the discrete problem, with primal objective of 442303 and GDT-TS score of 23.1. This is in contrast to our approach which finds the optimal and produces a primal objective of 217.7 and a GDT-TS score of 54.4. In the second experiment for each x_i we make a local set consisting of x_i^* as well as 4 points sampled with a Gaussian center on x_i^* . We only allow each x_i from the corresponding local point set. On this discrete graphical model, max-product indeed found the original solution with primal objective of 217.7 and GDT-TS score of 54.4. This demonstrates that particle max-product can find the solution when close to the optimal but suffers when a good initial estimate is not available.

As shown in Table 6 our approach results in more accurate predictions when using a hybrid representation with multiple templates. Table 3 shows the primal and dual values for the interval representation as a function of the number of voxels on a 10-node segment of the *1ctf* protein. As expected, the primal values of the interval convex max-product approach lower bound the MAP. When 15^3 voxels are used, the interval max-product converges with dual 0.28. Our particle method achieve a dual of 0.57. The interval max-product approach is very inefficient and a large set of voxels is needed to get a non-trivial lower bound. We believe using voxels of different sizes will improve efficiency, and we plan to investigate this in the future.

We finally compare our approach to particle max-product and MODELLER in the full dataset. As shown in Table 6 our approach outperforms significantly particle max-product (PBP), and performs comparably (better in 12 out of 20 proteins) to MODELLER. We believe this is a very promising result as MODELLER uses a much larger set of constraints than our approach, which employs a very simple energy function based only on distance constraints. We believe that exploiting the additional prior knowledge (i.e., physical constraints) that MODELLER utilizes, our approach will perform even better. Another interesting observation is that our method outperforms MODELLER in the harder proteins. The reason of this might be that the parameters of MODELLER are tuned to solve homology modeling for easy proteins

Table 4. Comparison to the baselines on 20 proteins ranging from 43 to 186 nodes and 788 to 16833 cliques. Our approach significantly outperforms Particle max product and performs comparably to MODELLER (Sali & Blundell, 1993), while only using a subset of the constraints.

Protein	length	#tem	MODELLER	PBP	Ours
T0437	99	1	61.6	32.7	60.9
T0451	133	2	64.3	27.8	67.1
T0464	89	1	42.3	28.7	44.1
T0471	133	2	57.1	31.2	57.9
T0473	68	1	90.4	42.1	88.9
T0522	134	2	94.4	32.4	93.2
T0562	123	1	33.5	25.5	35.7
T0574	126	2	55.1	31.2	57.8
T0579	124	1	42.9	26.8	44.1
T0592	144	2	73.5	25.8	72.3
T0606	123	1	69.5	32.6	69.1
T0610	186	1	69.8	28.7	66.2
T0622	138	2	60.5	30.5	62.5
T0630	132	1	54.4	22.8	56.2
1ctf	68	1	73.1	29.3	74.7
4icb	76	2	49.2	24.6	54.4
2cro	65	1	84.2	36.2	83.6
1fc2	43	1	64.2	27.9	67.8
2gb1	56	1	86.7	40.1	87.0
1enh	54	1	88.2	43.0	87.9

(Sali & Blundell, 1993).

7. Conclusion and Future Work

We have investigated convex belief propagation algorithms for Markov random fields (MRFs) with continuous variables. We have presented a theorem generalizing properties of the discrete case to the continuous case. We have derived an algorithm for computing the value of the Lagrangian relaxation of the MRF in the continuous case based on associating the continuous variables with an ever-finer interval grid. Finally, we have derived a particle method which uses convex max-product in re-sampling particles, and shown its effectiveness on the problem of protein folding.

References

- Bickson, D. Gaussian Belief Propagation: Theory and Application. *Arxiv preprint arXiv:0811.2518*, 2008.
- Cozzetto, D., Kryshafovich, A., Fidelis, K., Moul, J., Rost, B., and Tramontano, A. Evaluation of template-based models in CASP8 with standard measures. *Proteins*, 77 Suppl 9(S9), 2009.
- Eswar, N., Webb, B., Marti-Renom, M., Madhusudhan, M. S., Eramian, D., Shen, M., Pieper, U., and Sali, A. Comparative protein structure modeling using MODELLER. Chapter 2, November 2007.
- Folland, GB. *Real analysis: modern techniques and their applications*. Wiley-Interscience, 1999.
- Globerson, A. and Jaakkola, T. S. Fixing max-product: convergent message passing algorithms for MAP relaxations. In *NIPS*, 2007.
- Gront, D., Kmiecik, S., and Kolinski, A. Backbone building from quadrilaterals: a fast and accurate algorithm for protein backbone reconstruction from alpha carbon coordinates. *Journal of computational chemistry*, 28(9), July 2007.
- Hazan, T. and Shashua, A. Norm-Product Belief Propagation: Primal-Dual Message-Passing for Approximate Inference. *Arxiv preprint arXiv:0903.3127*, 2009.
- Hazan, T. and Shashua, A. Norm-Product Belief Propagation: Primal-Dual Message-Passing for Approximate Inference. *IEEE Transactions on Information Theory*, to appear, 2010.
- Ihler, A. and McAllester, D. Particle belief propagation. In *AISTATS*, 2009.
- Ihler, A.T., Frank, A.J., and Smyth, P. Particle-based variational inference for continuous systems. In *NIPS*, 2009.
- Kabsch, W. A solution for the best rotation to relate two sets of vectors. *Acta Crystallographica Section A*, 32(5), Sep 1976.
- Koller, Daphne, Lerner, Uri, and Angelov, Dragomir. A general algorithm for approximate inference and its application to hybrid bayes nets. In *UAI*, 1999.
- Meltzer, T., Globerson, A., and Weiss, Y. Convergent message passing algorithms—a unifying view. In *UAI*, 2009.
- Peng, J. and Xu, J. Low-homology protein threading. *Bioinformatics*, 26(12), June 2010.
- Rockafellar, R.T. *Convex duality and optimization*. Society for Industrial Mathematics, 1974.
- Sali, A. and Blundell, T. L. Comparative protein modelling by satisfaction of spatial restraints. *Journal of molecular biology*, 234(3), December 1993.
- Schlesinger, MI. Syntactic analysis of two-dimensional visual signals in noisy conditions. *Kibernetika, Kiev*, 4, 1976.
- Shimony, S.E. Finding MAPs for belief networks is NP-hard. *Artificial Intelligence*, 68(2), 1994.
- Simons, K. T., Kooperberg, C., Huang, E., and Baker, D. Assembly of protein tertiary structures from fragments with similar local sequences using simulated annealing and Bayesian scoring functions. *Journal of molecular biology*, 268(1), April 1997.
- Sontag, D. and Jaakkola, T. Tree block coordinate descent for MAP in graphical models. In *AISTATS*, 2009.
- Sontag, D., Meltzer, T., Globerson, A., Jaakkola, T., and Weiss, Y. Tightening lp relaxations for map using message passing. In *In Uncertainty in Artificial Intelligence (UAI)*, 2008.
- Sudderth, E.B., Ihler, A.T., Isard, M., Freeman, W.T., and Willsky, A.S. Nonparametric belief propagation. *CACM*, 53(10), 2010.
- Trinh, H. and McAllester, D. Unsupervised learning of stereo vision with monocular cues. In *BMVC*, 2009.
- Weiss, Y. and Freeman, W.T. Correctness of belief propagation in Gaussian graphical models of arbitrary topology. *Neural computation*, 13(10), 2001.
- Weiss, Y., Yanover, C., and Meltzer, T. Map estimation, linear programming and belief propagation with convex free energies. In *UAI*, 2007.
- Werner, T. A linear programming approach to max-sum problem: A review. *PAMI*, 29(7), 2007.
- Zemla, A., Venclovas, C., Moul, J., and Fidelis, K. Processing and analysis of CASP3 protein structure predictions. *Proteins*, Suppl 3, 1999.